Empirical decomposition of seismic response for soft soils

S.R. GARCIA[1], F.M. VILLALOBOS-CASTALDI[2], P. TREJO [3] & C. MARTÍNEZ [4]
[1, 3,4] Instituto de Ingeniería, Departamento de Geotecnia
Universidad Nacional Autónoma de México
[1]sgab@pumas.iingen.unam.mx
[3]PTrejoG@iingen.unam.mx
[4]CMartinezZ@iingen.unam.mx
[2]Grupo de Sistemas Inteligentes
Centro de Ciencias Aplicadas y Desarrollo Tecnológico,
Universidad Nacional Autónoma de México
miroslaba.villalobos@ccadet.unam.mx

Abstract: - In this paper the use of the Hilbert-Huang Transform (HHT), for the decomposition and characterization of seismic ground response, is discussed. The HHT, integrated by the Empirical Mode Decomposition (EMD) and the Hilbert Transformation (HT), enables engineers to analyze non-stationary oscillation systems and to obtain more detailed intensity descriptions on time-varying frequency diagrams. This paper uses the EMD to analyze recordings of accelerations of soft-soil deposits in Mexico City in order to detect and to describe the changes in the ground motion response patterns, as a result of extensive pumping to extract water from subsoil. Conclusions of the analysis of accelerograms indicate that the HHT is able to extract some motion characteristics useful in understanding the evolution of seismic responses of clayey soils, which might not be exposed effectively and efficiently by other conventional data processing techniques.

Keywords: - Hilbert-Huang Transform, Empirical Mode Decomposition, Time series analysis, Ground motions, Stiffening of clayey soils, Fundamental Period.

1 Introduction

Reliable earthquake characterization is essential to better understand local site effects related to seismic or man-made excitations. Faithful extraction and representation of seismic characteristics from motion recordings, together with other important features such as the energy distribution, frequencies content and duration of the movement, improve our knowledge of the underlying physical process the data expose.

Conventional approaches for analyzing dynamic and earthquake time series (accelerograms) (e.g., Fourier analysis, wavelets, and response spectra) can yield distorted, indirect, or incomplete information on the nature of the nonstationary time series from recordings, misleading the consequent use of these data in addressing many seismological and engineering issues.

This study proposes the use of the Hilbert-Huang Transform HHT (Huang et al., 1998), particularly its central part the Empirical Mode Decomposition EMD, for analyzing seismic recordings. Findings show that the EMD gives an advantageous well-defined description of the time-frequency energy content, and prove the validity and its great potential for engineering applications when dealing with nonstationary random processes. The subject of this study is the soil deposits in Mexico City. In this megalopolis the lacustrine environment propitiated the deposition of large volumes of fly ash and other pyroclastic materials that formed clays and clayey silts. These soils are notorious for their amazing power to amplify the waves traveling through the Earth's crust, as could be seen with the devastating effects of the 1985 earthquake (Michoacán earthquake, 19/09/1985).

In what follows we analyze responses from a recording Mexican station in order to obtain detailed information about behaviors patterns. Based on the results it is concluded that the EMD clarifies the nature of the responses and the effect that seismological and geotechnical situations have on the ground motions.

2 Hilbert-Huang Transform

In obtaining information from motion data, seismologists and engineers primarily use

transformed domain, time domain and response spectral analysis. Although these methods have shortcomings that are obviated by the HHT approach, it should be acknowledged that conventional data processing methods have merits that the HHT does not possess. Nevertheless, this study focuses on the advantages of the HHT in processing nonstationary data for certain types of information that the conventional methods might not be able to reveal effectively, directly, or completely (Huang and Shen, 2014).

The HHT was proposed by Huang et al, 1998, and consists of two parts: i) Empirical Mode Decomposition (EMD), and ii) Hilbert Spectral Analysis. In the EMD process, signals to be analyzed are adaptively decomposed into a finite number of intrinsic mode functions (IMFs). An IMF is described as a function satisfying the following conditions: i) the number of extrema and the number of zero-crossings must either equal or differ at most by one; and ii) at any point, the mean value of the envelope defined by the local maxima and the envelope defined by the local minima is zero. An IMF defined as above admits well-behaved Hilbert transforms. For an arbitrary function, X (t), in linear programming-class (Robert J.V., 2013), its Hilbert transform, Y (t) , is defined as

$$Y(t) = \frac{1}{\pi} P \int_{-\infty}^{\infty} \frac{X(t')}{t-t'} dt' \quad (1)$$

where P indicates the Cauchy principal value.

Consequently an analytical signal $Z(t)$, can be produced by

$$Z(t) = X + iY(t) = a(t)e^{i\theta(t)} \quad (2)$$

where

$$a(t) = [X^2(t) + Y^2(t)]^{1/2},$$

and

$$\theta(t) = arctan\frac{Y(t)}{X(t)} \quad (3)$$

are the instantaneous amplitude and phase of $X(t)$, respectively.

Since Hilbert transform $Y(t)$ is defined as the convolution of $X(t)$ and $1/t$ by Eq. (1), it emphasizes the local properties of $X(t)$ even though the transform is global. In Eq. (2), the polar coordinate expression further clarifies the local nature of this representation. Using Eq.(2), the instantaneous frequency of $X(t)$ is defined as

$$\varpi(t) = \frac{d\theta(t)}{dt} \quad (4)$$

However, there is still considerable controversy on this definition. A detailed discussion and justification can be found in (Huang et al., 1998). Applying the EMD process, any signal $X(t)$ can be decomposed into finite IMFs, $imf_j(t)$ $(j= 1,...n)$ $j =$, and a residue $r(t)$ (r indicates the signal tendency), where n is nonnegative integer depending on $X(t)$, i.e.,

$$X(t) = \sum_{j=1}^{n} imf_j(t) + r(t) \quad (5)$$

For each $imfj$, let $X(t) = imf_j(t)$, its corresponding instantaneous amplitude, $a_j(t)$, and instantaneous frequency, $\varpi_j(t)$, can be computed with Eqs. (3) and (4). By Eqs. (2) and (4), imf_j can be expressed as the real part RP in the following form:

$$imf_j(t) RP|a_j(t)\exp(i\int w_j(t)dt| \quad (6)$$

Therefore, by Eqs. (4) and (5), $X(t)$ can be expressed as the IMF expansion as follows,

$$X(t) = RP\sum a_j(t)\exp(i\int \varpi_j(t)dt) + r(t) \quad (7)$$

which generalize the following Fourier expansion

$$X(t) = \sum_{j=1}^{\infty} a_j e^{iwjt} \quad (8)$$

by admitting variable amplitudes and frequencies. Consequently, its main advantage over Fourier expansion is that it accommodates non-stationary data perfectly. Eq. (7) enables us to represent the amplitude and the instantaneous frequency as functions of time in a three-dimensional plot, in which the amplitude is contoured on the time-frequency plane. The time-frequency distribution of amplitude is designated as the Hilbert amplitude spectrum or simply Hilbert spectrum, denoted by $H(\varpi, t)$. Having obtained the Hilbert spectrum, the marginal spectrum is defined as follows:

$$h(\varpi) = \int_0^T H(\varpi, t)dt \quad (9)$$

The marginal spectrum offers a measure of total amplitude (or energy) contribution from each frequency value. For details and a deeper mathematical explanation see (Huang and Shen, 2104).

3 Hilbert-Huang Transform of Earthquake Recordings

To illustrate the HHT analysis technique for studying earthquakes –transient signals (Anderson, 1991), data from the September 19th 1985 earthquake, recorded in SCT site (Lake Zone of Mexico City) are analyzed. The original accelerogram (E-W component) is shown in Fig. 1.a and its corresponding Fourier amplitude spectrum in Fig. 1.b. The Fourier spectrum indicates that the frequency content of the waves is spread out with the maximum spectral amplitudes at 0.1 and 1 Hz. In contrast, the EMD depicted in Fig. 1.c reveals important characteristics of the waves with just a few IMF components. Examination of Figure 1.c indicates that the first components (IMF1 and IMF2) and the last ones (IMF7 to IMF11) with negligible amplitudes represent noise and the numerical error in the EMD process. On other hand, modes IMF3 to IMF6 can be considered as the true seismic waves.

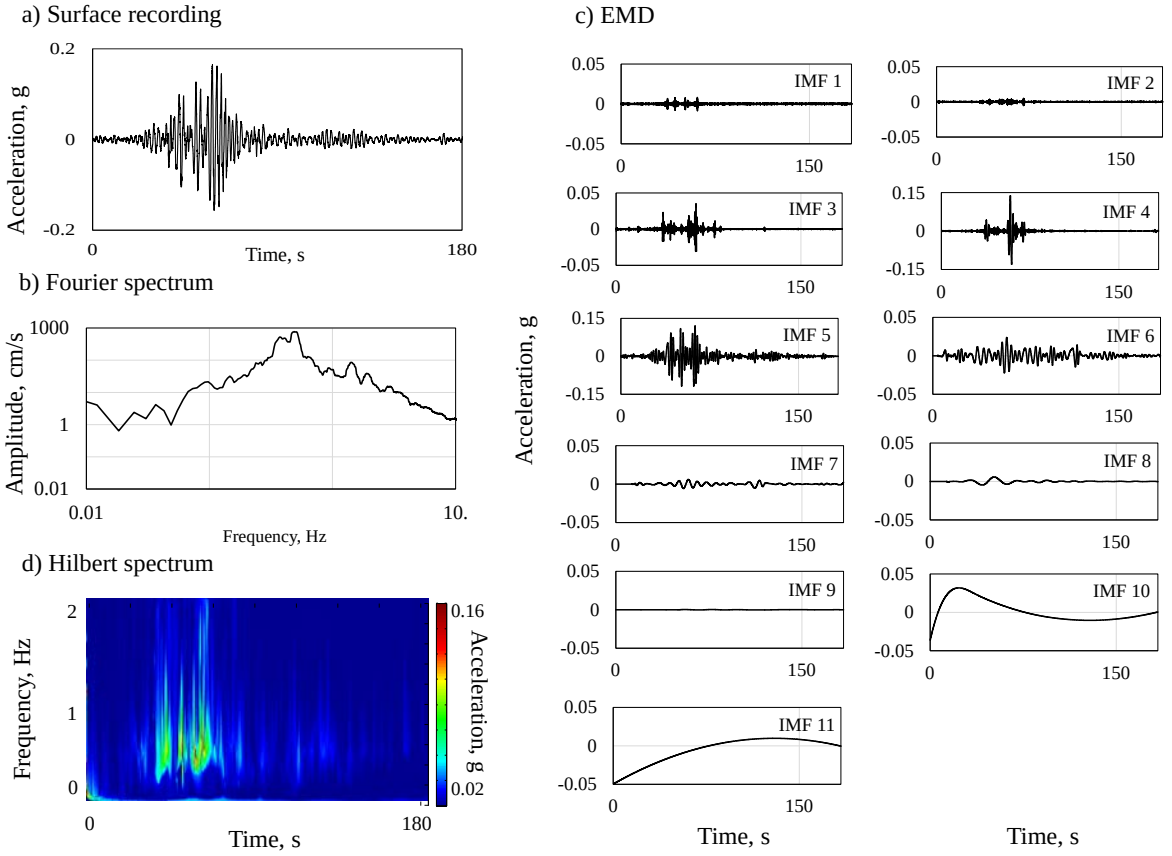

Figure.1 HHT analysis of the September 19th 1985 earthquake, SCT site.

The Hilbert spectrum (Fig. 1.d) shows a clear picture of temporal-frequency energy distribution. A set of strong-ground motions is recognized in the time interval of 50-80, implying just one event of response directly related with the rupture process.

Characteristics of peak amplitude, waveform, and frequency content of this set of waves, can help reveal quantitative differences in the seismic source mechanism and in potential nonlinear soil responses. Iso-intensity zones in Fig. 1.d expose that the event has the most important energy levels around an instant frequency of 0.5 Hz (at ~70 s) but medium levels, that cannot be neglected, activate instant frequencies up 1.5 Hz.

From the viewpoint of structural engineering, this kind of set of waves will cause much larger dynamic responses than one that does not cover a wide range of frequencies, even though the peak amplitudes could be comparable. Singling out the low frequency wave signals and knowing the temporal-frequency energy distribution observed in the acceleration data, some aspects about source mechanism and extent of potential nonlinear soil response, as well as in low-frequency pulse-like influences on long-period structures, can be

quantified. The Fourier amplitude spectrum, as indicated before, does not provide truthful information of low-frequency waves nor concerning the time-dependent or evolutionary frequency content.

4 Changes in geotechnical conditions

Geotechnical engineers in Mexico City have studied systematically its subsoil for many decades. In most of the area formerly occupied by the lakes, main soil formations are ordered in a sequence of soft clay strata interspersed with lenses and layers of harder clayey silts with sands. As seen in the stratigraphical cross-section of Fig. 2, the main soil strata are (a) archaeological debris and fills, the uppermost materials, (b) a crust of desiccated low plasticity silty clays, (c) the Upper Clay Formation having the most compressible soils, (d) the first Hard Layer that appears at an average depth of about 40 m, formed by sands, gravelly sands and thin lenses of softer silty clays, (e) the Second Clay Formation, about 10m thick, and (f) the so called Deep Deposits—very consistent silts and sandy silts interspersed with hard clays—appear at the base of the stratigraphical column (50m deep or so).

In response to water extraction and the ensuing consolidation process, effective stresses will increase and, consequently, the properties of the clay strata that underlie the former lake bed will change. In what follows we present evidence of these changes, taken from the results of soundings performed in different dates at several sites in the city and from the results of tests performed on soil samples retrieved from several places within the former lake bed. Effective stress increments also affect dynamic soil properties and the seismic response of the soft lacustrine clays will also change, as discussed here.

The evolution of pore pressures, measured over a 10 year period, illustrate the gradual depletion of pore pressures at a site in the central part of the city. Pore pressure decay rates varied from 0.002 to 0.014 kPa/year at different depths and at different times, over the 1990–2002 period. Also the water content, volumetric weight and undrained strength profiles at two different dates (1952 and 1986) (Fig. 3) for a site located within a densely urbanized zone, where earthquake related damages have concentrated recurrently in the past, shows that (a) thicknesses of the relevant clay strata have reduced as a consequence of regional subsidence; (b) water content reductions are especially significant below 15m approximately which is consistent with the fact that pumping induced consolidation propagates upwards from the base of the clayey soils to the surface; (c) changes in soil density (volumetric weight) and in undrained strength confirm that soil strata densify and gain strength as the clay masses consolidate regionally.

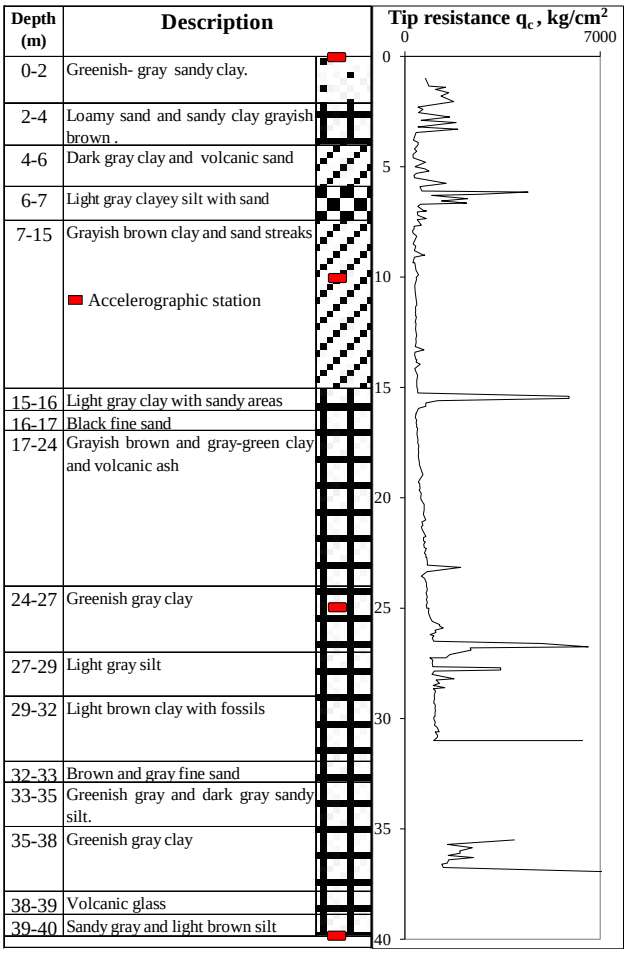

Fig 2. Stratigraphical column in SCT site

The most dramatic change is observed in dynamic properties. In this respect we look at the evolution on shear wave propagation velocities, shear moduli and damping ratios. Field evidence of changes on shear wave velocities is given in Fig. 4, from the results of suspension logging tests performed in 1986 and 2000 also at the SCT site [1], the expected stiffening of the clay strata over the 15 years that lapsed between the two dates is more evident for greater depths. The samples obtained in 2001 were taken from the same stratum as the 1986 samples. In both sets of experiments the samples were consolidated to the same range of isotropic consolidation pressures.

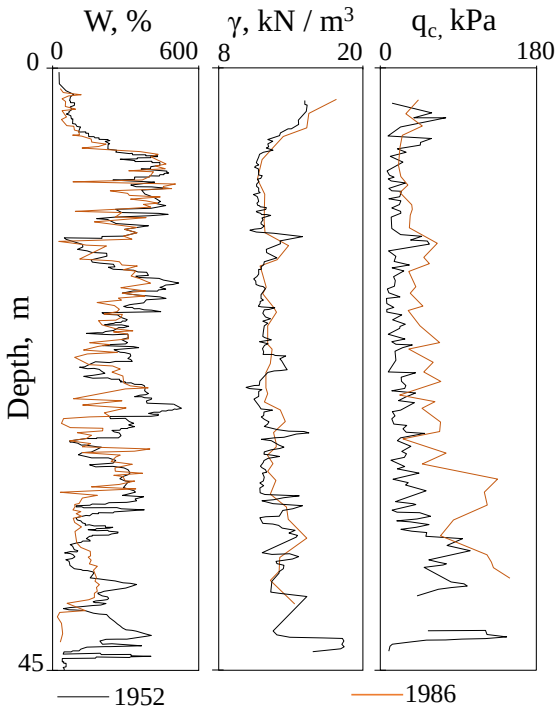

Fig. 3 Water content W, volumetric weight γ and undrained strength q_c profiles

5 Empirical Modes of Seismic Soil Response

The effects of regional subsidence on the seismic response of Mexico City clay deposits are illustrated by studying one location within the lake zone in Mexico City, the SCT site, where accelerographic stations have been in operation since the 1970s. In order to view how seismic response changes as water is pumped from the deep aquifers, it is necessary to study: i) the changes in the dynamic soil properties, which, as shown before, are related to increments in effective stress (brought about during the regional consolidation process) and ii) the accelerations registered over the same years period. In this research the results from the study of earthquakes recordings will be presented.

The data set explored consisted of a series of 22 accelerations time series recorded during earthquakes that happened from 1985 to 2011.

The characteristics of these events are enlisted in Table 1. The signals are of 150 s length (on average), at a measuring rate of 0.01s. According with the procedure described above (EMD algorithm) the accelerograms were decomposed into their IMF components. The results are like those shown, by way of example, in Fig. 5 (IMFs obtained from the recording of the 30th September 1999, epicenter in Oaxaca coast). For this accelerogram the algorithm yielded 9 components plus a residue. The nine IMFs has clear characteristics, in amplitude and in frequency content that may not be related to sinusoidal signals.

For the whole data set, the number of IMFs needed to decompose the signals fluctuates from 8 to 12 modes what is in agreement with empirical recommendations (Wu et al., 2001). Using the EMD the local variation of ground motions can be precisely detected and the meaning of the intrinsic oscillations can be related to the phenomena without restrictive hypothesis. The conclusions obtained from the behavior of each mode are more *natural* than those achieved from theoretical positions faraway the system which generates the signal.

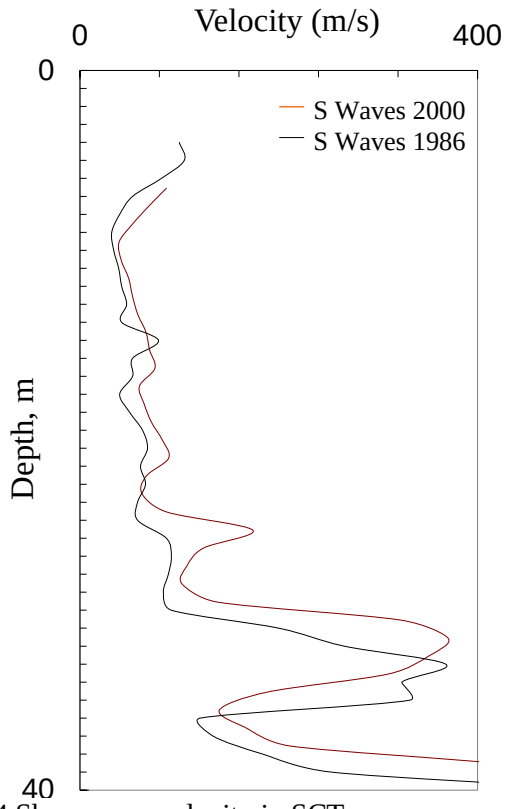

Fig. 4 Shear wave velocity in SCT

To validate that the decomposition was performed correctly and, at the same time, discriminating between modes, a proof of completeness is necessary. Simply adding modes, from the first to the last, one by one, it is verified that the integration of IMFs re-constructs the original signal. For illustrating the procedure, the summing is applied to the recorded accelerogram and its IMFs shown in Fig. 5. As can be seen in Fig. 6, the sum of the first modes plus the residue is far from resembling the original signal but when modes 3, 4 and 5 are added practically the recorded ground motion has been reassembled.

Table 1. Characteristics of seismic events

No.	Date	Magnitude	Epicenter		Focal depth	Epicentral distance
			LAT. N	LONG. W	km	km
1	19/09/1985	8.1	18.081	102.942	15	425
2	02/12/1985	3	19.300	99.286	1	17
3	04/01/1986	5.4	19.530	107.980	9	928
4	05/01/1986	3.5	19.410	99.440	< 5	31
5	24/10/1993	6.6	16.540	98.980	19	315
6	23/05/1994	5.6	18.030	100.570	23	212
7	10/12/1994	6.3	18.020	101.560	20	296
8	15/07/1996	6.5	17.450	101.160	20	302
9	11/01/1997	6.9	17.910	103.040	16	442
10	22/05/1997	6	18.410	101.810	59	305
11	19/07/1997	6.3	15.860	98.350	5	400
12	20/04/1998	5.9	18.370	101.210	66	245
13	15/06/1999	7	18.180	97.510	69	219
14	21/06/1999	6.2	17.990	101.210	54	267
15	30/09/1999	7.6	15.950	97.030	16	442
16	29/12/1999	6.1	18.020	101.680	82	307
17	21/07/2000	6	18.090	98.970	48	145
18	09/08/2000	7	17.990	102.660	16	402
19	08/10/2001	6.1	16.940	100.140	4	291
20	22/01/2003	7.6	18.600	104.220	9	540
21	26/04/2011	5.5	16.710	99.690	7	302
22	05/05/2011	5.5	16.610	98.910	11	309

Continue adding modes 6, 7, 8 and 9 does not substantially modify the signal obtained in the previous step. This procedure was applied to the whole dataset and the completeness was confirmed for each individual. As a result, it could be verified that, with minimal differences between the original signals and the sum of the components, summing the first five IMFs leads to the original accelerograms.

To grow deeper in the study of the IMFs and to use the findings for describing the ground motions, it is necessary to typify them with metrics used in geotechnical and seismological engineering.

5.1 Peak ground acceleration PGA and Maximum instant amplitude MIA

PGA is equal to the maximum ground acceleration that occurred during earthquake shaking at a location and it is equal to the amplitude of the largest absolute acceleration recorded on an accelerogram at a site during a particular earthquake (Campbell, K.W. et al., 2003).

In an earthquake, damage to buildings and infrastructure is related more closely to ground motion, of which PGA is a measure, rather than the magnitude of the earthquake itself.

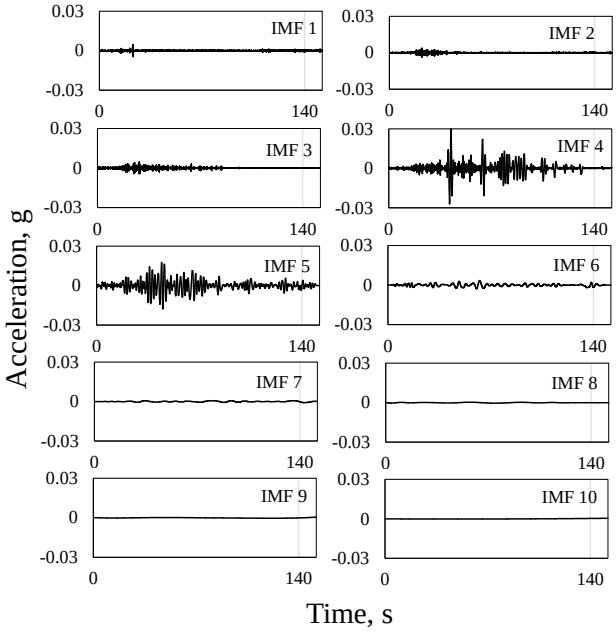

Fig 5. IMFs obtained from the September 30th, 1999 event

Fig. 7 shows the boxplot of the maximum instant amplitudes MIA related to the number of IMFs for the whole data set. As can be seen, components IMF1 to IMF3 have lesser MIAs if compared with the contribution of IMF4 and IMF5 to the maximum ground acceleration registered in signals. MIAs in last components, IMF6 to IMF10, are minimal so it can be said that these oscillations do not contribute to ground response and are negligible. It is important to mention that the extraordinaire 1985 Michoacán earthquake, M8.1, follows this trend of behavior. The observed difference lies only in MIAs intensity but the central modes, IMF4 and IMF5, is maintained. It seems that the recognized non-linear effect of the intensity of seismic input on the response of soft soils (Bazurro and Cornell, 2004), does not change the most important intrinsic oscillation.

For the studied phenomenon and analyzed population, there is one particular IMF, the IMF5, that seems contains the higher MIAs levels.

This vital mode is recurrent regardless of the magnitude of the earthquake, the generation mechanism, the distance from the epicenter to the measurement point (SCT site), even it has not changed in the ~30 years of registration in which it is said, the site has undergone remarkable variations in stiffness due to pumping.

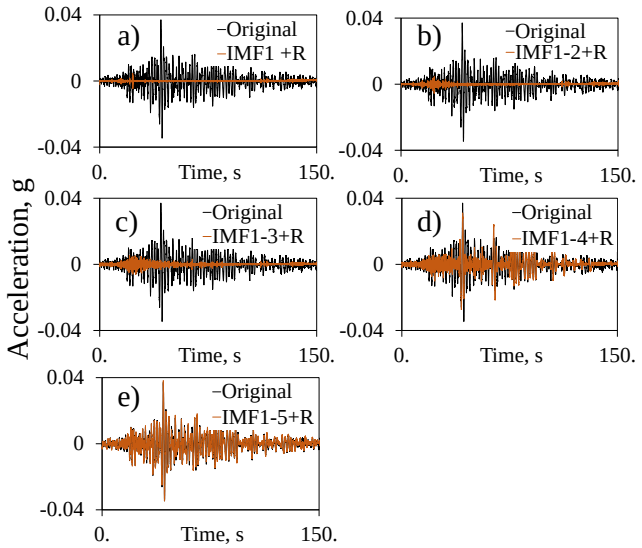

Fig. 6 Proof of completeness of the September 30th, 1999 event.

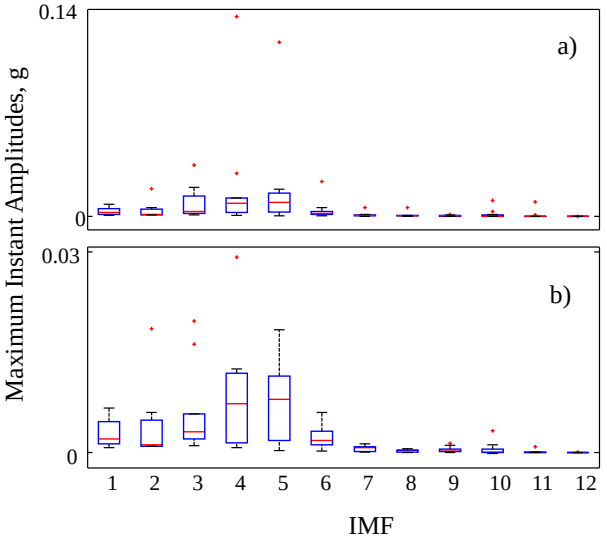

Fig. 7 Boxplot of MIAs according to the IMF, a) including the 19/09/85 Michoacán earthquake, b) including M≤7.5.

This finding basically indicates that, despite the soil properties alterations, the deposit has a unique, central, intrinsic oscillation.
We proposed in this investigation, and is the object of a further research, that the IMF5 may be associated with the mode in which the compressible, plastic, with high water content, clayey soils vibrate. This could mean that intrinsically the clay deposits has a "seed" motion, a core oscillation pattern, and the differences in recorded responses because of urban surroundings, generation mechanism, magnitude, epicentral distance and/or directivity may have effect on modes IMF1 to IMF4.

The level of MIAs responses as the seismic input is more or less severe (observing M and epicentral distance) is clearly represented in the boxes of modes IMF4 and IMF5, thus the boxes of other modes (IMF1 to IMF3) suggest that the nature of these oscillations may be due to other vibrating sources, possibly buildings and urban ambient.

5.2 Fundamental period and Instant frequency

Several past earthquake events have resulted in devastating failures of built environment, which in most of the cases are attributed to strong amplification of seismic waves. As earthquake energy propagates through soil media, its amplification or attenuation is mainly related to fundamental natural period T_n of the soil deposit.
The fundamental period of a soil deposit is dependent on its thickness, low strain stiffness and density. Estimation of these characteristics has been the subject of several research studies, yet inconsistencies and uncertainties associated with their estimation have not been resolved conclusively. Hence, many researchers tend to corroborate their calculations by indirect characterization of soil deposits using data recorded in surface and downhole array of instruments during earthquake events. The theoretical procedures for determining the natural period lead to closed solutions but none of these methods is free from drawbacks and controversies in T_n estimation.
The best tactic to establish the fundamental period of a soil deposit is to compute it using an abstract method and then compare this value with that exposed by recorded data. For soft soil deposits in Mexico City the more general and accepted approach to calculate T_n is to interpret the Lake zone as homogeneous soil deposits overlying a rigid bedrock, with constant shear wave velocity profiles throughout its depth H (Kramer, 1996). Then, the natural period T_n corresponding to n^{th} mode of vibration is given by $T_n = 4H/(2n-1)V_s$. Hence natural period T corresponding to fundamental mode (n = 1) is given by,

$$T_n = \frac{4H}{V_s} \qquad (10)$$

Since $V_s = \sqrt{G/\rho}$, where G is the soil shear modulus and ρ is the density, the above equation may be expressed as $T = 4H\sqrt{\rho/G}$. This means that the stiffening of the soil deposit must have a tangible immediate effect on the value of

fundamental period or fundamental frequency. Theoretically fundamental natural period for SCT (entire soil deposit, from 0.0 m until fist hard layer, at ~40m) calculated using average of shear wave velocity method is T_n = 2.0s (or fundamental frequency f_n=0.5 Hz). Using the microtremors (Lermo and Chávez-García, 1994) and MDOF *Multi Degree of Freedom System* method (Bozorgnia and Bertero, 2004) the computed T_n the values occur in the vicinity of the above, slightly higher, T_n~2.1s.
In order to relate the central modes and the concept of fundamental natural period, we analyzed every IMF for all the events in the data set and obtained the predominant frequency f_n (frequency where maximum spectral amplitude is reached) from their Fourier spectra. In Fig.8 a boxplot of the f_n variation corresponding to each IMF is depicted. As can be observed, the frequency value progressively decays as the mode number increases.

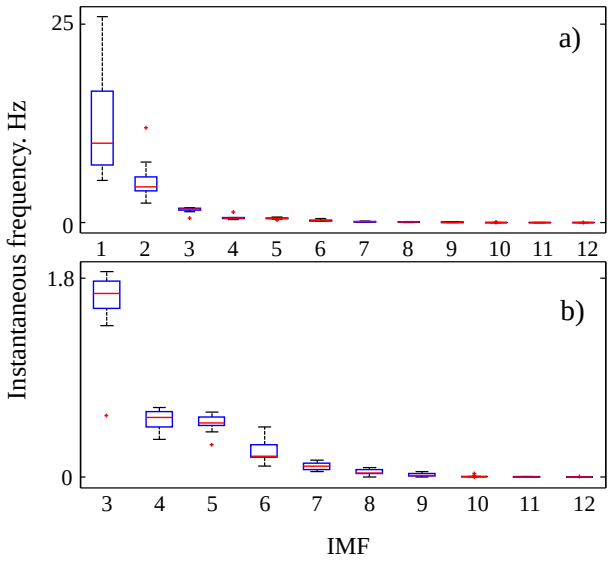

Fig. 8 Boxplot of f_n, a) including the twelve modes, b) excluding the first two modes, frequencies content not related to soils vibrating.

One conclusion from the MIA analysis is that the last modes, those after IMF5, could be eliminated because of their negligible amplitude (see Fig. 7), this assumption is reinforced analyzing frequencies because of their very low f_n values (near to zero) reported from IMF6 to IMF12.
The first modes (IMF1 and IMF2) have frequency ranges that cannot be related to soft soil responses so, despite of their MIAs, they were removed from the ground motion analysis. Nevertheless we cannot ignore that for the completeness proof these two modes are very significantly to the reconstruction of the original signal so they will be examined separately later.

Subsequently the IMF3, IMF4 and IMF5 are the individuals considered for the ground motion analysis. Observing the f_n trends and the MIAs of these three modes, *natural* relations between the recorded responses and oscillations emerged.
IMF3 can be easily associated with the T_2 or f_2 of the soil deposit (Fig. 9).

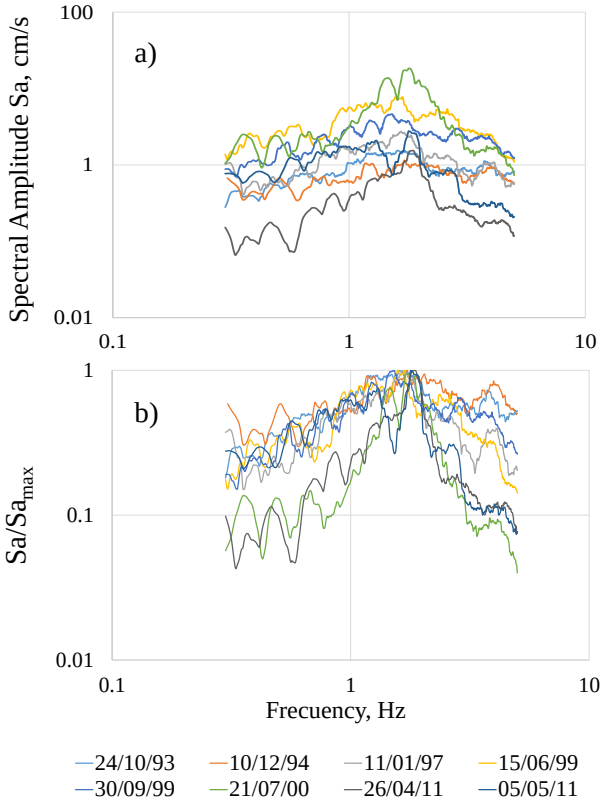

Fig. 9 IMF3 extracted from selected events.

This second vibration mode has been evaluated using the MDOF method (Lermo and Chávez-García, 1994) and its value, ~1.4 Hz, is very similar to the f_n of the IMF3. Note that the differences between the responses are because of the intensity of the seismic waves traveling through the soil deposit (directly related with the energy from the seismic source). The secondary frequency f_2 stays despite of the generator mechanism, focal depth, directivity and aging. Events registered and exposed in the Fig. 10 cover a time period of 30 years and signs of substantial changes in frequencies of soils vibrating, or some of evident stiffening, cannot be found. What is clear is the division between spectral shapes from M<5.5 and M≥5.5 events.
In Fig.10 the IMF4 behavior is depicted. In this case it is not straightforward to detect the f_n from the spectra, however some modes (those obtained from accelerograms recorded during subduction events) have a natural frequency around 0.5 Hz what is very

close to the f_1 of SCT, but there are examples, those from intraplate events, that have natural frequencies ~1.4 Hz.

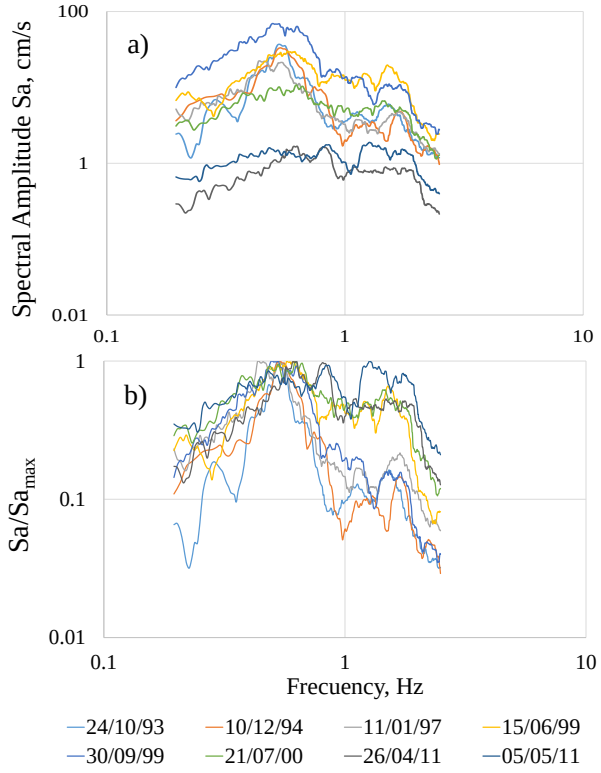

Fig. 10 IMF4 extracted from selected events.

The variations between responses are, as in the IMF3 analysis, dependent on the magnitude of seismic event and two categories are detected: i) spectral shapes for M≥5.5 with f_n ~1.4 Hz and ii) spectral shapes for M<5 with f_n ~0.5 Hz. Between these classes the respective natural frequency remains despite of generator mechanism, focal depth, directivity and the time period among recordings. Again, evidence of stiffening (shift to the right of the fundamental frequency) cannot be found.

Based on the characteristics of the spectra of IMF5 (Fig.11) it is corroborated that this mode can be seen as the oscillation that better represent the "seed" motion and because of that, the fundamental period of the soil deposit. The f_n in the spectra is undoubtedly identified with ~0.5 Hz (T_n= 2.0 s). See the narrow band that they formed when are normalized (scaled versions with respect to its maximum spectral amplitude). Because of their good fit to a single envelope this f_n can be labeled as distinctive of IMF5, despite of the kind of event (intraplate or interplate), focal depth, magnitude, epicentral distance, directivity, urban environment and/or stiffening of soils. Because there are no variations in spectral shape and the differences are detected exclusively in spectral amplitudes we assumed that the central oscillation only reacts to the intensity of seismic waves (bedrock input) and to the combination of other effects, increasing the value of spectral amplitudes.

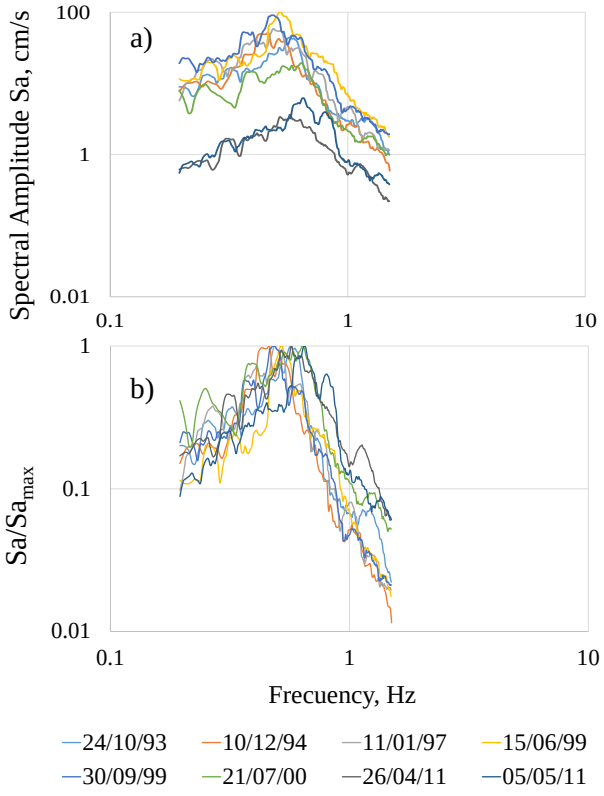

Fig. 11 IMF5 extracted from selected events.

Then, if the hypothesis that the stiffening of the soil deposit has an effect on the fundamental period or fundamental frequency would be correct, and verifying that the *true* oscillations, the IMF5s, have not changed their response path (analyzed f_n or T_n) during these ~30 years of observations we can point that: i) the effect of the stiffening is still so light that it cannot be observed yet through the apparatus, possibly because of their recording capacity, ii) the amount of urban-ambient noise is so high that is masking the *true* ground motions behavior, or iii) the changes in dynamic properties, in this stage of the pumping process, affect the amplification capacity of the soil deposit more clearly on number of times than what they do on the fundamental frequency.

It is important to mention that the first modes (IMF1 and IMF2) with f_n that cannot be related to vibration modes in soft soils (higher frequencies than those reported for very plastic and compressible clays) have MIAs that should be considered in the analyses

of seismic response. Finding the source of these oscillations, with constant amplitudes and frequencies throughout the records, could help to explain the differences between the responses and behaviors predicted or expected (by numerical models and by the intuition of engineers) and those registered in the accelerographic stations during the most recent earthquakes.

5 Conclusions

This study introduces the method of HHT for earthquake data analysis and investigates its rationale for studies of geotechnical earthquake engineering and seismology. The decomposed components in EMD of HHT, namely, the IMF components, may contain observable, physical information inherent to the ground motions.

Despite of static and dynamic soil properties in the SCT site have changed and will continue to do on account of regional subsidence brought about by water pumping from the deep aquifers, it seems that there are still many knowledge gaps in i) determining the aptitude of the recordings for analyzing specific response trends, ii) selecting the more appropriate time-series analysis techniques and, therefore, iii) validating the process of calibration the theoretical models.

The findings of this research do not lead to conclusive evidence on the effects of stiffening clays, it cannot be quantitatively presented. It is mandatory to keep studying the earthquake motions in order to prevent the undesirable consequences of misunderstood the soil properties and seismic responses.

References:

Jens H., Gerardo A. (2015), Instrumentation in Earthquake Seismology, Springer, pp 413.

García, S.R., H. Solís-Estrella, K. Ramírez-Amaro, F. Correa, S. García, J. Figueroa-Nazuno, y A. Angeles-Yreta, (2005) Descomposición Empírica en Modos: una interpretación sísmica, Memorias del XV Congreso Nacional de Ingeniería Sísmica. Mexico.

Gomez, B., A., (2002). “Interpretation of Soil Effect at Mexico City Valley Using Accelerograph High Density Arrays”, Ph. D. Thesis. Facultad de Ingeniería, Universidad Autónoma de México, México. (In Spanish).

Huang, N. E., Shen, Z. and Long S. R., (1998), The empirical mode decomposition and the Hilbert spectrum for nonlinear and non-stationary time series analysis. Proc. R. Soc. Lond. A, pages 903–995.

Huang, N. E., Shen, Z, (2015), Interdisciplinary Mathematical Sciences, Volume 16 Hilbert–Huang Transform and Its Applications, Norden E Huang, USA, pp 400.

Robert J.V. (2013), Linear Programming: Foundations and Extensions, International Series in Operations Research & Management Science 196, Springer Science & Business Media, pp 414.

Zhang, R., Ma S., Hartzell S., (2003), Signatures of the seismic source in EMD-based characterization of the 1994 Northridge, California, earthquake recordings, Bull. Seismol. Soc. Am. 93 (1), 501–518.